

## Symmetry of Two-Terminal Nonlinear Electric Conduction

A. Löfgren,<sup>1</sup> C. A. Marlow,<sup>2</sup> I. Shorubalko,<sup>1</sup> R. P. Taylor,<sup>2</sup> P. Omling,<sup>1</sup> L. Samuelson,<sup>1</sup> and H. Linke<sup>2,\*</sup>

<sup>1</sup>*Solid State Physics and The Nanometer Consortium, Lund University, Box 118, S-22100 Lund, Sweden*

<sup>2</sup>*Materials Science Institute and Physics Department, University of Oregon, Eugene, Oregon 97403-1274, USA*

(Received 11 August 2003; published 29 January 2004)

The well-established symmetry relations for linear transport phenomena cannot, in general, be applied in the nonlinear regime. Here we propose a set of symmetry relations with respect to bias voltage and magnetic field for the nonlinear conductance of two-terminal electric conductors. We experimentally confirm these relations using phase-coherent, semiconductor quantum dots.

DOI: 10.1103/PhysRevLett.92.046803

PACS numbers: 73.63.Kv, 73.23.Ad, 73.50.Fq

Symmetries with respect to the sign of a bias voltage and the direction of an applied magnetic field  $B$  are central to our understanding of electron transport phenomena. In the linear response regime, the Onsager-Casimir relations  $\sigma_{\alpha\beta}(B) = \sigma_{\beta\alpha}(-B)$  describe these symmetries in terms of the local conductivity tensor [1]. These relations were derived for macroscopic, disordered solid-state conductors where the conductor boundaries are unimportant. In mesoscopic samples, the characteristic length scales for elastic and inelastic (phase-breaking) scattering can exceed the dimensions of the device. In this limit a local description of transport is not possible, and the reciprocity theorem  $R_{12,34}(B) = R_{34,12}(-B)$  must be used [2,3]. For two-terminal conductors, the reciprocity theorem reduces to  $G_{12}(B) = G_{12}(-B)$ , where  $G_{12}$  is the conductance with the current flowing from contact 1 to 2. The sign of the source-drain bias voltage and the orientation of the measurement leads are of no consequence in the linear response regime, such that  $G_{12}(B) = G_{21}(B)$ .

The reciprocity theorem breaks down in the nonlinear response regime [4–7]. In the general case, where the conductor has no symmetry (e.g., due to disorder),  $G_{12}(V) \neq G_{12}(-V)$ . This is because, if an applied voltage modifies the asymmetric device potential, the resulting device potential depends on the voltage sign [6–8]. Similarly, no symmetries with respect to magnetic field are expected for an asymmetric device, that is,  $G_{12}(V, B) \neq G_{12}(V, -B)$  (for an illustration, see Fig. 1).

While the general breakdown of the reciprocity theorem in the nonlinear transport regime is well known [4–7], a systematic evaluation of surviving symmetries in this regime has not previously been attempted. It is the point of this Letter to establish a complete set of symmetry relations for the nonlinear conductance of two-terminal conductors. One important motivation is that the nonlinear regime is fundamental to applications of submicron electronic devices, for which linear response is limited to very small voltages [4,5].

In the following, we consider conductors without significant disorder. We first propose a set of general symmetry relations with respect to bias voltage and magnetic

field for the nonlinear electric conductance. We show that symmetry of nonlinear transport requires geometrical symmetry of the conductor—a substantial experimental challenge in terms of fabrication and material quality. Using purposely designed semiconductor quantum dots, we then demonstrate that the symmetry relations are experimentally observed and that deviations from perfect geometrical symmetry can be measured.

Without loss of generality, we consider triangular conductors because of their simple geometrical shape. We refer to a device as left-right (LR) symmetric when it possesses a symmetry axis perpendicular to the current direction and up-down (UD) symmetric when it possesses a symmetry axis parallel to the current direction. We consider the symmetry of the nonlinear electrical conductance under reversal of voltage, magnetic field, and lead orientation. In this context it is important to note that in a real experimental setup the reversal of voltage ( $V \rightarrow -V$ ) is not generally equivalent to physically interchanging the leads attached to the probes ( $G_{12} \rightarrow G_{21}$ ), because the circuit used to measure the conductance may itself be asymmetric. For instance, the gate voltage  $V_g$  used to electrostatically define the conductor's shape is usually set with respect to the drain contact on one side of the device, breaking the circuit symmetry. When appreciable source-drain voltages are used, the resulting gradient in the local electrochemical

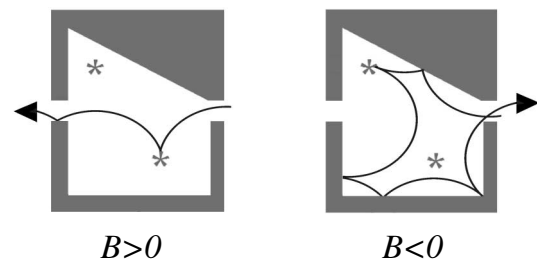


FIG. 1. Schematic electron trajectories for positive and negative magnetic fields. In the absence of symmetry in a mesoscopic device, the conductance is not expected to be symmetric with respect to the direction of a magnetic field, when a bias voltage defines a source and a drain contact.

potential along the conductor deforms the device potential defined by the gate in a way that depends on the voltage sign. This can lead to circuit-induced asymmetry (CIA) of the conductance even when the device itself is LR symmetric [9–11]. In order to avoid CIA, special care must be taken in the device design [12]. Here we focus on so-called “rigid” devices, in which CIA is not significant, and refer the reader to Ref. [11] for a discussion of devices that are not rigid.

For rigid devices, regardless of their symmetry, a voltage reversal is equivalent to swapping source and drain leads, such that

$$G_{12}(V, B) = G_{21}(-V, B) \quad (\text{rigid}). \quad (1)$$

This relation is illustrated in Fig. 2 (compare, for instance, configurations A and G or D and F).

For the special case of rigid devices that are LR symmetric, we expect

$$G_{12}(V, B) = G_{12}(-V, -B) \quad (\text{LR, rigid}). \quad (2)$$

Equation (2) holds independent of whether or not the device is UD symmetric, but is not expected if LR symmetry is absent. This can be seen by comparing, for instance, A and D or B and C in Fig. 2.

UD symmetry implies that, for a given voltage, reversal of a magnetic field perpendicular to the device plane should be of no consequence for electron transport [8]:

$$G_{12}(V, B) = G_{12}(V, -B) \quad (\text{UD}). \quad (3)$$

This can be seen by comparing, for instance, A and B in Fig. 2. Note, however, that the absence of LR symmetry implies that in the nonlinear regime  $G_{12}(V) \neq G_{12}(-V)$ , regardless of the magnetic field sign [5,7,8]. Equation (3) does not involve a reversal of lead orientation or voltage

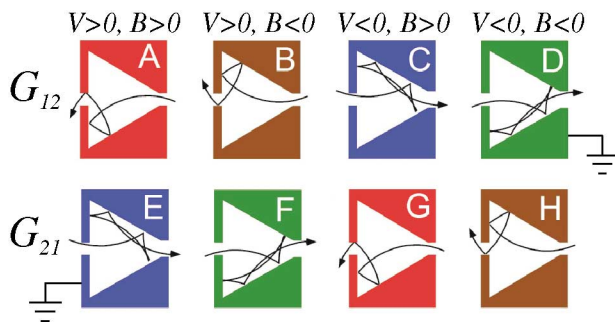


FIG. 2 (color). Illustration of the symmetry relations expected for a rigid device in the nonlinear regime and at finite magnetic field. The upper and lower rows show the two possible lead configurations  $G_{12}$  and  $G_{21}$ , distinguished by the position of the grounding point relative to the device. Different classical electron trajectories illustrate the difference in transmission probability that results when the potential depends on the sign of the voltage applied to the source contact. Positive magnetic field is taken to be into the page.

sign and is therefore valid for both rigid and nonrigid devices.

Finally, we note that the conductance of a LR-symmetric device (regardless of rigidity and UD symmetry) is expected to be invariant upon reversal of lead orientation and of the external magnetic field:

$$G_{12}(V, B) = G_{21}(V, -B) \quad (\text{LR}). \quad (4)$$

Relationships (1)–(4), the first main result of our Letter, are based on fundamental symmetry arguments and are therefore expected to hold in both the classical and quantum regimes of transport. In order to test these relationships, we used ballistic semiconductor devices defined by deep wet etching in modulation-doped, 9 nm thick InP/GaInAs quantum wells. The devices were of equilateral-triangular shape with a side length of 1  $\mu\text{m}$ , smaller than the electrons’ elastic mean free path of 6.1  $\mu\text{m}$  and smaller than the phase-coherence length  $l_\phi = 3.5 \mu\text{m}$  at  $T = 230 \text{ mK}$  and  $V = 0$  ( $l_\phi = 1.7 \mu\text{m}$  at  $T = 230 \text{ mK}$  and  $V = 3 \text{ mV}$ ). In this phase-coherent regime of electron transport, the wavelike nature of the carriers leads to conductance fluctuations (CF) as a function of an applied magnetic field. Because of their origin in wave interference, and because of the short Fermi wavelength (30 nm), details of the CF are known to be sensitive to the exact shape of the potential forming the device and to defects or impurities [13]. Phase-coherent measurements of CF are therefore particularly well suited to test the influence of device geometry and of disorder on the conductance symmetry. Contact openings used to measure the conductance were positioned such that either UD-symmetric (Fig. 3) or LR-symmetric (Fig. 4) quantum dots were formed. Two-terminal magnetoconductance measurements were carried out in four-point geometry. A small ac signal (rms amplitude 20  $\mu\text{V}$ , comparable to  $kT \approx 20 \mu\text{eV}$ ) was added to a tunable dc bias voltage  $V$ . The differential conductance  $g_{ij} = dI_{ij}/dV_{ij}$  was measured using lock-in techniques in order to reduce measurement noise. We checked that there was no significant non-Ohmic behavior in the circuit.

Figure 3 shows  $g_{ij}$  for a bias voltage  $|V| = 1 \text{ mV} \approx 50kT/e$  as a function of a perpendicular magnetic field for an UD-symmetric, triangular quantum dot [14]. The eight traces shown are individual measurements taken over the course of 2 days in the eight possible configurations of sign of the bias voltage, direction of the magnetic field, and lead orientation (see Fig. 2). As expected for a device lacking LR symmetry, the CF are not symmetric in  $V$ , as we note from a comparison of Figs. 3(a) and 3(b) or Figs. 3(c) and 3(d) [15]. However, for a rigid device, Eq. (1) predicts that reversal of the leads and bias voltage should lead to identical CF, regardless of the device symmetry. The similarity of traces shown in the same color (for instance, A and G or D and F) qualitatively

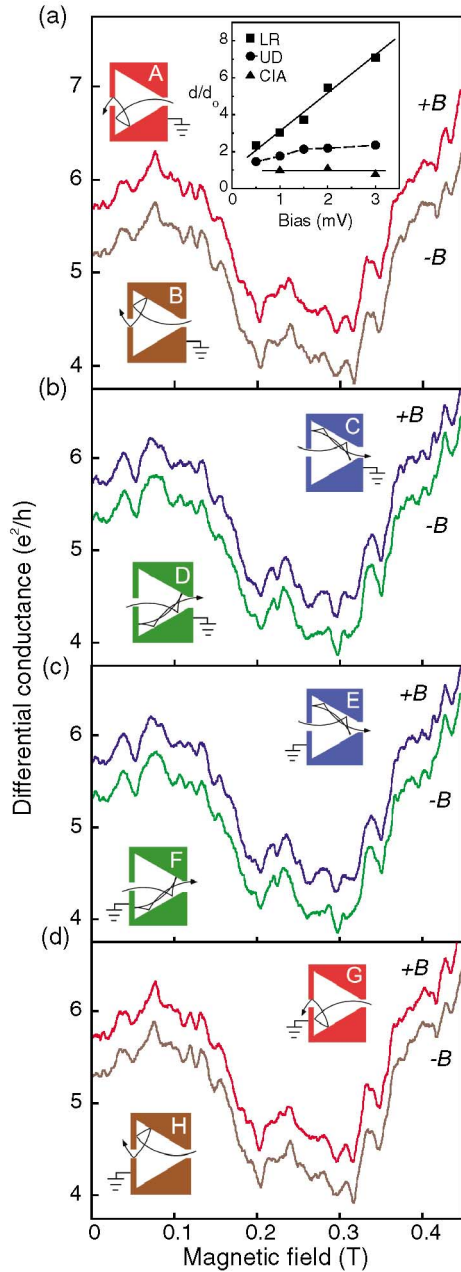


FIG. 3 (color). Magnetoconductance fluctuations for an UD-symmetric quantum dot measured in the eight possible different configurations of lead orientation, sign of bias voltage, and sign of magnetic field (capital letters refer to the panels in Fig. 2): (a)  $g_{12}(V = +1 \text{ mV}, \pm B)$ , (b)  $g_{12}(V = -1 \text{ mV}, \pm B)$ , (c)  $g_{21}(V = +1 \text{ mV}, \pm B)$ , and (d)  $g_{21}(V = -1 \text{ mV}, \pm B)$ . The lower trace in each panel has been offset by  $-0.5e^2/h$  for clarity. The inset in (a) shows  $d_{LR}/d_0$ ,  $d_{UD}/d_0$ , and  $d_{CIA}/d_0$  as a function of  $V$  (lines are guides to the eye).

verifies Eq. (1) and shows that the device used in Fig. 3 can be regarded as rigid [12].

According to Eq. (3), in the presence of perfect UD symmetry conductance fluctuations should be unaltered when the direction of the magnetic field is reversed. This prediction can be tested by comparing the pairs of traces

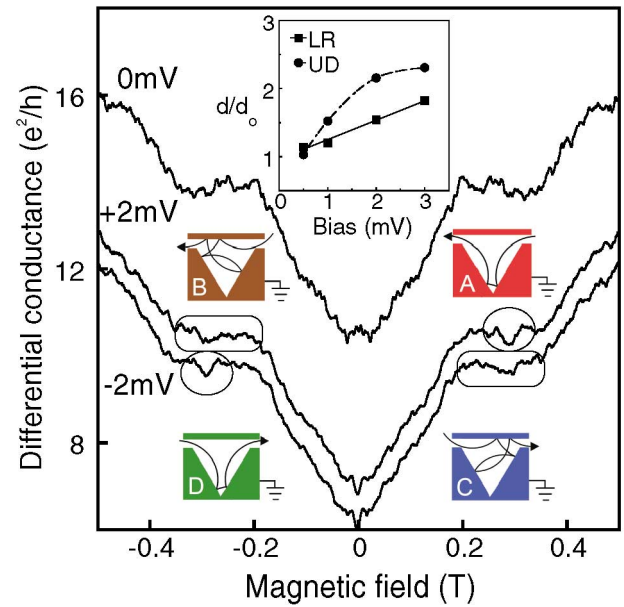


FIG. 4 (color). Magnetoconductance fluctuations  $g_{12}(V, B)$  of a LR-symmetric device for  $V = 0$ ,  $V = +2 \text{ mV}$ , and  $V = -2 \text{ mV}$  (capital letters in each measurement configuration refer to the corresponding panel in Fig. 2). Data are offset for clarity. Note that  $g_{12}(V, B) \neq g_{12}(V, -B)$ , while  $g_{12}(V, B)$  and  $g_{12}(-V, -B)$  show very similar features, as predicted by Eq. (2) (see, e.g., the marked features). Inset:  $d_{LR}/d_0$  and  $d_{UD}/d_0$  as a function of  $V$  ( $d_0 = 4.21 \times 10^{-2} e^2/h$  for this device). Lines are guides to the eye.

in the individual panels in Fig. 3 (e.g., A and B or C and D). Again, striking similarities are observed.

In order to quantify the difference between two magnetoconductance traces, say, the difference  $d_{AB}$  between traces  $g_A(B)$  and  $g_B(B)$  measured in configurations A and B, respectively, we determine the root mean square (rms) of their difference, using  $10^3$  data points spaced by 0.5 mT between  $B = 0$  and  $B^{\max} = \pm 0.5 \text{ T}$ :

$$d_{AB} = \sqrt{\frac{1}{B^{\max}} \int_0^{B^{\max}} [g_A(B) - g_B(B)]^2 dB}. \quad (5)$$

The value  $d_{AB} = 0$  would correspond to identical traces. To calibrate the influence of experimental noise and setup instabilities on  $d$ , we use two CF traces recorded 2 days apart in nominally identical configurations ( $V = 0$ ). Separately evaluating  $d$  for the traces recorded for positive and negative magnetic field and then averaging the results, we find  $d_0 = 2.99 \times 10^{-2} e^2/h$ , a value comparable to experimental noise ( $\approx 0.5\%$ ) of the device conductance. In comparison, the four pairs of traces that should be identical if the device is rigid (A–G, B–H, C–E, D–F) yield an averaged value of  $d_{CIA} = (d_{AG} + d_{BH} + d_{CE} + d_{DF})/4 = 3.10 \times 10^{-2} e^2/h$  and  $d_{CIA}/d_0 = 1.04$ . A comparison of data sets that, according to Eq. (2), should be the same if the device was LR

symmetric (A–D, B–C, E–H, F–G), yields  $d_{LR}/d_0 = 3.05$ . In comparison, a test for UD symmetry (A–B, C–D, E–F, G–H) yields the averaged value  $d_{UD}/d_0 = 1.77$ . In other words, the intentional absence of LR symmetry in the device geometry causes the largest conductance asymmetry, while unintentional deviations from UD symmetry, such as material and fabrication imperfections, have a significantly smaller, but measurable effect. The effect of CIA in our devices is not significant compared to experimental noise, confirming that the device is rigid. Note, however, that CIA can be substantial in other devices, for instance, in some surface-gated devices [9,10,12].

The inset in Fig. 3(a) shows the quantified asymmetries (normalized to  $d_0$ ) as a function of increasing bias voltage. Consistent with a first order nonlinear effect,  $d_{LR}$  increases approximately linearly with bias voltage. On the other hand,  $d_{UD}$ , which is attributed to imperfections in the UD symmetry of the device, which are not expected to change with voltage, increases only weakly with  $V$ . At all voltages used, the influence of CIA remained insignificant compared to the noise level ( $d_{CIA}/d_0 \approx 1$ ).

For comparison with the UD-symmetric device discussed so far, in Fig. 4 we show CF for the LR-symmetric device. Whereas at  $V = 0$  (linear regime) the conductance is symmetric in  $B$ , at finite  $V$  (nonlinear regime) each of the two data traces taken is not symmetric in  $B$ , due to the absence of UD symmetry. However, one can see by comparing the marked conductance features that  $g_{12}(V, B) \approx g_{12}(-V, -B)$ . This observation confirms Eq. (2) and indicates that the device is rigid, consistent with our conclusion about the UD-symmetric device. We therefore expect that any  $d_{LR}$  observed should be due to unintentional deviations from LR symmetry. Indeed, at all bias voltages used  $d_{LR}/d_0$  for this device (see inset in Fig. 4) is substantially smaller than for the LR-asymmetric device used in Fig. 3. As one would expect intuitively from the symmetry of the device, for small bias  $d_{LR}$  is also smaller than  $d_{UD}$  (inset in Fig. 4). Note, however, that the values found for  $d_{UD}/d_0$  in the UD- and the LR-symmetric devices are comparable, highlighting an interesting open question: At present, no theoretical prediction about the dependence of  $d_{UD}$  on disorder, magnetic field, or bias voltage is available. Our data [see insets in Figs. 3(a) and 4] suggest a sublinear increase of  $d_{UD}$  with  $V$  and little sensitivity to the amount of intentional asymmetry.

In summary, we have demonstrated, using a sensitive experimental test, a set of novel symmetry relations for the electric conductance of mesoscopic devices in the nonlinear regime and in the presence of a magnetic field. Our prediction of these symmetry relations is based on symmetry arguments. A natural next step would be a rigorous theoretical study along the lines of Ref. [3] and applicable to the nonlinear regime of transport.

The authors thank P. E. Lindelof for useful discussions, I. Maximov for lithography, and W. Seifert for crystal growth. This work was supported by NSF IGERT, the ONR, the Swedish Foundation for Strategic Research, the Swedish Research Council, and the Research Corporation.

\*Corresponding author.

Email address: linke@uoregon.edu

- [1] L. Onsager, Phys. Rev. **38**, 2265 (1931); H. B. G. Casimir, Rev. Mod. Phys. **17**, 343 (1945).
- [2] M. Büttiker, Phys. Rev. Lett. **57**, 1761 (1986).
- [3] M. Büttiker, IBM J. Res. Dev. **32**, 317 (1988).
- [4] B. L. Al'tshuler and D. E. Khmel'nitskii, JETP Lett. **42**, 359 (1985); T. Christen and M. Büttiker, Europhys. Lett. **35**, 523 (1996).
- [5] R. Landauer, in *Nonlinearity in Condensed Matter*, edited by A. R. Bishop *et al.* (Springer-Verlag, Berlin, 1987).
- [6] R. A. Webb, S. Washburn, and C. P. Umbach, Phys. Rev. B **37**, 8455 (1988); S. B. Kaplan, Surf. Sci. **196**, 93 (1988); P. G. N. de Vegvar *et al.*, Phys. Rev. B **38**, 4326 (1988); R. Taboryski *et al.*, Phys. Rev. B **49**, 7813 (1994); P. A. M. Holweg *et al.*, Phys. Rev. Lett. **67**, 2549 (1991); D. C. Ralph, K. S. Ralls, and R. A. Buhrman, Phys. Rev. Lett. **70**, 986 (1993).
- [7] H. Linke *et al.*, Europhys. Lett. **44**, 341 (1998).
- [8] H. Linke *et al.*, Phys. Rev. B **61**, 15914 (2000).
- [9] N. K. Patel *et al.*, Phys. Rev. B **44**, 13549 (1991).
- [10] A. Kristensen *et al.*, Phys. Rev. B **62**, 10950 (2000).
- [11] A. Löfgren *et al.* (to be published).
- [12] CIA is important when the variation of the conductance with gate voltage is comparable to other nonlinear effects, that is, when  $\partial G/\partial V_g \approx \partial G/\partial V$  [10,11]. Our devices were defined by deep wet etching rather than by surface gates. Furthermore, a Ti/Au top gate used to tune the carrier concentration was separated from the quantum well by a  $1\ \mu\text{m}$  layer of insulating polymer, and  $\partial G/\partial V_g \approx 0.6 (e^2/h)/V$  was 1–2 orders of magnitude smaller than in typical, surface-gated GaAs/AlGaAs devices.
- [13] W. J. Skocpol *et al.*, Phys. Rev. Lett. **56**, 2865 (1986).
- [14] It can be shown that any symmetry relation in  $V$  or  $B$  that holds for  $G_{ij}$  must also hold for  $g_{ij}$  [11].
- [15] The CF are superimposed onto a broad background that is due to classical commensurability effects [16]. While the phase-sensitive CF show nonlinear behavior at very small voltages, significant classical nonlinear effects are not (in the absence of CIA) expected until several millivolts, where electron orbits are changed by the applied voltage. However, at those higher voltages the sensitive CF are suppressed due to heating effects. We therefore limit our study to voltages up to 2 mV.
- [16] H. Linke *et al.*, Phys. Rev. B **56**, 1440 (1997).